Multiscale Modeling of Magnetic Materials: Temperature-dependence of the Exchange Stiffness

U. Atxitia[1], D. Hinzke[2], O. Chubykalo-Fesenko[1], U. Nowak[2], H. Kachkachi[3], O. N. Mryasov[4], R. F. Evans[5], R. W. Chantrell[5]

[1] *Instituto de Ciencia de Materiales de Madrid, CSIC, Cantoblanco, 28049 Madrid, Spain*

[2] *Department of Physics, University of Konstanz, 78457 Konstanz, Germany*

[3] *LAMPS, University of Perpignan Via Domitia,*
52 avenue Paul Alduy,, 66860 Perpignan cedex, France

[4] *Center for Materials and Information Technology,*
University of Alabama, Tuscaloosa, AL, U. S. A. and

[5] *Department of Physics, University of York, York YO10 5DD, U. K.*

For finite-temperature micromagnetic simulations the knowledge of the temperature dependence of the exchange stiffness plays a central role. We use two approaches for the calculation of the thermodynamic exchange parameter from spin models: (i) based on the domain wall energy, (ii) based on the spin-wave dispersion. The corresponding analytical and numerical approaches are introduced and compared. A general theory for the temperature dependence and scaling of the exchange stiffness is developed using the classical spectral density method. The low-temperature exchange stiffness A is found to scale with magnetization as $m^{1.66}$ for systems on a simple cubic lattice and as $m^{1.76}$ for an FePt Hamiltonian parametrized through *ab initio* calculations. The additional reduction of the scaling exponent, as compared to the mean-field theory ($A \sim m^2$), comes from the non-linear spin-wave effects.

I. INTRODUCTION

Micromagnetic modeling has proved to be a very useful tool, complementary in many respects to experimental measurements, especially for calculations of hysteresis and dynamics of magnetic nanoelements such as magnetic grains, dots, stripes etc.[1-5]. Nowadays the micromagnetic approach is used as a design tool, for example, for the evaluation of novel magnetic recording media performance[6]. The importance of micromagnetics can hardly be overestimated since a huge amount of experimental work in nanomagnetism relies on the physical insights provided by micromagnetic modeling, based, for example, on open source programs such as OOMMF[7] or Magpar[4]. Micromagnetic modeling needs as input fundamental magnetic (micromagnetic) parameters: effective crystalline anisotropy K, exchange stiffness A and saturation magnetization M_s. These are provided normally by experimental measurements as sample averaged quantities. The dynamics is based on the integration of the classical Landau-Lifshitz-Gilbert (LLG) equation of motion which requires additional input parameters such as the Gilbert damping constant.

On the other hand, *ab initio* models has turned out to be efficient in providing insight on the local atomic scale values such as the local magnetic moment μ_s, the local anisotropy d or a pair-wise exchange J_{ij} in nanoclusters or periodic cells[8,9]. Most of the *ab initio* calculations are zero-temperature, and the *ab initio* modeling of finite temperature magnetization dynamics in nanoscale magnetic elements remains still a challenge for the future.

At the same time, standard micromagnetics is also essentially zero-temperature, although the micromagnetic parameters could be taken as experimentally measured values at a given temperature T. In "thermal micromagnetics" the fluctuations are introduced as additional random fields acting on each discretization element[10,11]. It has been shown that this approach is correct only for low temperatures[12] due to the fact that the standard micromagnetic approach considers constant magnetization length in each element. Thus high-frequency spin waves (SW), responsible for longitudinal magnetization fluctuations near the Curie temperature T_c are cut off and the value of the Curie temperature is strongly overestimated. An improved micromagnetic approach for higher temperatures is based on the Landau-Lifshitz-Bloch (LLB) equation[13,14] which removes the condition of the conservation of the magnetization magnitude at each discretization element and introduces longitudinal fluctuations.

The modern approach combines the strength of both methods in a unique multi-scale modeling scheme[15], where information from the *ab initio* to the micromagnetic scale is used. The correct account for thermal fluctuations is provided by using an intermediate atomistic scale (classical Heisenberg models[15] parameterized through *ab initio* calculations). These models are known for their suitability to evaluate thermodynamic properties at any temperature. Here the thermal fluctuations are introduced via a Metropolis Monte Carlo algorithm or by means of the Langevin dynamics approach[16].

The multiscale scheme proposed in Ref. 15 proceeds as follows. Ab-initio calculations are mapped onto an atomistic spin model based on a classical Heisenberg Hamiltonian[8,9,15]. The atomistic model is used to evaluate the temperature dependent parameters $K(T)$, $M_s(T)$ and the longitudinal and transverse susceptibilities which

are the physical parameters required for the LLB equation. This provides a direct link from the electronic structure lengthscale to a mesoscopic, single spin equation of motion capable of large scale simulations. However, the use of large scale (micromagnetic) models requires the temperature dependence of the micromagnetic exchange constant $A(T)$. The evaluation of temperature dependent macroscopic parameters is highly non-trivial. While the temperature dependence of the anisotropy constant as well as its scaling behavior with the temperature-dependent magnetization $M(T)$ is known (analytically at least at low temperature and for simple systems, see e. g.[17]; for a more general numerical method within the multiscale scheme, see Ref.18.) the temperature dependence of the exchange stiffness has received little attention. Atxitia et al[19] employed a quadratic scaling law $A(T) \propto M(T)^2$, which is essentially a mean field result. However, given the importance of this parameter in micromagnetic calculations, a more detailed investigation is strongly justified.

In the present article, we investigate the temperature dependent exchange stiffness $A(T)$ in detail. In order to get a thorough understanding of its temperature-dependence as well as its scaling with magnetization we use different methods and models for our investigation. Our methods are based on classical definitions of the exchange stiffness: through the domain wall (DW) and through the spin wave (SW) approaches. The development of the methods also provides a basis for future multiscale modelling theory where the temperature dependence of the parameters cannot be expected to follow simple laws and should be numerically evaluated. The paper is organized as follows. Firstly we outline the atomistic model which forms the basis of the calculations. The model is then used to calculate $A(T)$ using a method based on the domain wall stiffness. This is followed by a mean-field treatment of the problem. The atomistic model is then used to calculate $A(T)$ based on the SW stiffness. Interestingly the two methods (DW stiffness and SW stiffness) give essentially the same scaling law, demonstrating the link between the two phenomena. It is also shown that the scaling exponent can be material dependent. Finally we present analytical calculations using a classical spectral density method. This model is shown to give a scaling law in agreement with the numerical results and, importantly, to give a scaling law for the anisotropy constant in agreement with experiment and with previous numerical simulations, demonstrating the power of the analytical model.

II. MODELS

Our models are based on the classical Heisenberg Hamiltonian. To investigate the generality of our approach, in what follows we use two types of model systems: (i) a generic Heisenberg Hamiltonian for localized magnetic moments on a simple cubic lattice and (ii) a specific Hamiltonian for FePt, parameterized through *ab initio* calculations[8].

The generic ferromagnet is described by the Hamiltonian

$$\mathcal{H} = -\mu_\mathrm{s}\mathbf{H} \cdot \sum_{i=1}^{\mathcal{N}}\mathbf{S}_i - d\sum_{i=1}^{\mathcal{N}}(S_i^z)^2 - \frac{1}{2}J\sum_{\langle i,j \rangle}\mathbf{S}_i \cdot \mathbf{S}_j \quad (1)$$

where $\mathbf{S}_i$, with $|\mathbf{S}_i| = 1$ and $i = 1,\ldots,\mathcal{N}$, are classical spins, $J > 0$ is the ferromagnetic exchange constant, in the following restricted to nearest-neighbors, μ_s is the atomistic magnetic moment, $\mathbf{H} = H\mathbf{e}_z$ is the external magnetic field, d is the on-site magnetic anisotropy parameter, and $\mathcal{N}$ is the number of spins in the system.

FePt is intensively investigated due to its potential application as ultra-high density recording media[20]. In previous publications[8] bulk FePt was modeled in the layered $L1_0$ phase. The model has been constructed on the basis of first-principles calculations of non-collinear (finite angle) configurations calculated using constrained local spin density functional (LSDA) theory[21], infinitesimal angle or LSDA based perturbation theory[22–24] and site-resolved magneto-crystalline anisotropy with beyond LSDA corrections[25]. The fundamental interactions at the electronic level are strongly modified by the $L1_0$ structure. In particular it was shown[8] that the Fe moments can be considered as localized, while the Pt induced moments have to be treated as essentially delocalized. Nevertheless, it is possible to construct a classical spin Hamiltonian involving only the Fe degrees of freedom, with the introduction of a two-ion anisotropy term and a modified exchange term[8]. This Hamiltonian was used in several theoretical studies[26–28] and was verified by a comparison of the temperature dependence of the anisotropy constant with experimental data[8,29,30].

In the following, we consider the full Hamiltonian, described in detail in Ref.[8] including Zeeman energy and dipole-dipole coupling,

$$\begin{aligned}\mathcal{H} = \;& -\sum_{i<j}\left(J_{ij}\mathbf{S}_i \cdot \mathbf{S}_j + d_{ij}^{(2)}S_i^z S_j^z\right) - \sum_i d^{(0)}(S_i^z)^2 \\ & -\sum_{i<j}\frac{\mu_0\mu_\mathrm{s}^2}{4\pi}\frac{3(\mathbf{S}_i\cdot\mathbf{e}_{ij})(\mathbf{e}_{ij}\cdot\mathbf{S}_j)-\mathbf{S}_i\cdot\mathbf{S}_j}{r_{ij}^3} - \sum_i \mu_\mathrm{s}\mathbf{H} \cdot \mathbf{S}_i. \end{aligned} \quad (2)$$

The two-ion anisotropy parameters $d_{ij}^{(2)}$ represent the dominant contribution to the uniaxial anisotropy energy as compared to the single-ion term $d^{(0)}$. The exchange interactions J_{ij} (and consequently also $d_{ij}^{(2)}$) are taken into account up to a distance of 5 unit cells until they are finally small enough to be neglected. Note that all parameters follow from SDFT calculation so that the model contains no adjustable parameters.

The zero-temperature exchange stiffness $A(0\,\mathrm{K})$ can be easily evaluated from local values J_{ij} and the interatomic distances. When the exchange energy between spins is written for the small angle deviations, the classical exchange energy in terms of the continuous magneti-

sation vector $\mathbf{m}$ takes the form

$$\mathcal{E}_{\text{ex}} = \sum_{ij} J^{ij} \left((\mathbf{a}_{ij} \cdot \nabla) \mathbf{m} \right)^2 = \sum_{\nu} A_{\nu} \int \left[(\nabla m_{\nu})^2 \right] d\mathbf{r}, \tag{3}$$

where the first summation is over the position vectors $\mathbf{a}_{ij} = \mathbf{r}_i - \mathbf{r}_j$ from lattice point i to all its neighbors, $\nu = x, y, z$ and the "classical micromagnetic exchange stiffness" at zero temperature is

$$A_{\nu}(0\text{K}) = \frac{1}{V_0} \sum_{ij} (J_{\nu}^{ij}/2)(a_{ij}^{\nu})^2, \tag{4}$$

where V_0 is the volume of the unit cell. The direct summation of the exchange gives $A_{x(y)}(0\text{K}) = 1.13 \times 10^{-11} \text{J/m}$ for the exchange stiffness perpendicular to Fe planes and $A_z(0\text{K}) = 2.37 \times 10^{-11} \text{J/m}$ within Fe planes in agreement with the results of Ref. 27.

Since we are interested in thermal properties we use Langevin dynamics, i. e., simulations of the stochastic Landau-Lifshitz-Gilbert (LLG) equation of motion. This equation has the form

$$\frac{(1 + \alpha^2)\mu_{\text{s}}}{\gamma} \dot{\mathbf{S}}_i = -\mathbf{S}_i \times \mathbf{H}_i(t) - \alpha \, \mathbf{S}_i \times \left(\mathbf{S}_i \times \mathbf{H}_i(t) \right), \tag{5}$$

with the gyromagnetic ratio $\gamma = 1.76 \times 10^{11} (\text{T}s)^{-1}$ and a dimensionless Gilbert damping parameter α which we set to $\alpha = 1$ (high damping limit) in the domain wall stiffness approach (section III) and to $\alpha = 0.1$ in the spinwave stiffness approach (section IV). Note that the value of the damping parameter does not influence thermal equilibrium properties[31], only the dynamics of the system. The large value for α we chose guarantees fast relaxation to thermal equilibrium and will not influence our results since we are only interested in equilibrium properties.

Thermal fluctuations are included as an additional noise term $\zeta_i(t)$ in the internal field $\mathbf{H}_i(t) = -\frac{\partial \mathcal{H}}{\partial \mathbf{S}_i} + \zeta_i(t)$, with $\langle \zeta_i(t) \rangle = 0$ and $\langle \zeta_i^k(t) \zeta_i^l(t`) \rangle = 2\delta_{ij}\delta_{kl}\delta(t - t`)\alpha k_{\text{B}} T \mu_{\text{s}}/\gamma$, where i, j denote lattice sites and k, l the Cartesian components. All algorithms we use are described in detail in Ref. 16.

In the following we use two physical definitions of $A(T)$ based on the domain wall stiffness and the spin-wave stiffness parameter. Numerical calculations are extended using a Mean-Field approach and a classical spectral density method.

III. THE DOMAIN WALL STIFFNESS APPROACH

A. Numerical approach: Thermodynamic Exchange Stiffness

In the present section, we evaluate the exchange stiffness from the temperature dependent free energy of a domain wall and its corresponding width. For this purpose

we perform Langevin dynamics simulations for a generic Heisenberg model as well as for the FePt Hamiltonian. For the generic model we use a system of 32^3 moments. For FePt the system size has a cross section of 25.6×25.6 nm^2 and a length of 12.8 nm. This was found sufficiently large to avoid finite size effects. In both systems we create a domain wall by applying fixed, antiparallel boundary conditions.

The free energy ΔF of the domain wall is obtained from numerical calculations of the internal domain wall energy ΔE, which is the energy difference between a system with and without a domain wall, using the relation

$$\Delta F(\beta) = \frac{1}{\beta} \int_0^{\beta} \Delta E(\beta') d\beta'. \tag{6}$$

where $\beta = 1/k_B T$, k_B is the Bolzmann constant and T is the temperature. It is found that domain wall profiles are well described by the usual hyperbolic functions[32], so that we were able to fit the domain wall width δ. Assuming that the well-known equations for the domain wall width,

$$\delta(T) = \pi \sqrt{\frac{A(T)}{K(T)}}, \tag{7}$$

and the free energy,

$$\Delta F(T) = 4\sqrt{A(T) \, K(T)}, \tag{8}$$

hold even at finite temperature, we can obtain the micromagnetic exchange stiffness $A(T)$ as well as the anisotropy energy constant $K(T)$. For a more detailed description of the applied methods see[27,28].

The results obtained for the scaling behavior of $A(m)$ are shown in Fig.1 for the generic model and in Fig. 2 for the FePt model. A scaling behavior, $A(m) \propto m^{\kappa}$, is found at low temperatures. The values for κ will be discussed later on in connection with the SW stiffness approach.

B. Theory: Mean-field approximation

To gain a further insight into the thermodynamic behavior of exchange stiffness we performed also mean-field (MF) calculation. A one-dimensional domain wall is considered, where the magnetization is uniform within planes. We start with the Hamiltonian of a generic ferromagnet given in Eq.(1), on a simple cubic lattice with nearest-neighbor interactions only and in zero anisotropy and magnetic field. The MF Hamiltonian has the form

$$\mathcal{H}_{\text{MF}} = - J \sum_i \mathbf{S}_i \cdot (\mathbf{m}_{i-1} + 4\mathbf{m}_i + \mathbf{m}_{i+1})$$
$$+ \frac{J}{2} \sum_i \mathbf{m}_i \cdot (\mathbf{m}_{i-1} + 4\mathbf{m}_i + \mathbf{m}_{i+1}), \tag{9}$$
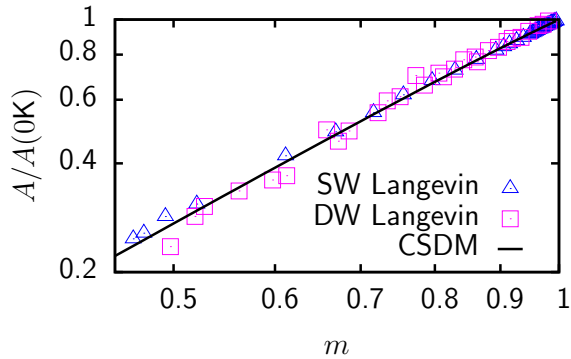
Figure 1: Scaling behavior of the exchange stiffness (DW Langevin) as obtained from the domain wall free energy for a generic model with $d/J = 0.032$. The solid line is the numerical solution of the CSD method outlined in section IV.B. The SW Langevin points are obtained from the SW stiffness approach based on the atomistic LLG-Langevin simulations outlined in section IV.A
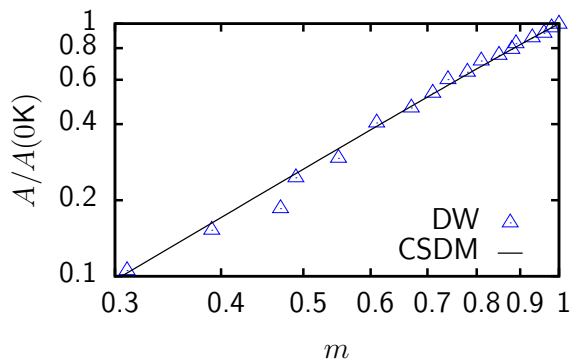

Figure 2: Scaling behavior of the exchange stiffness as obtained from the DW method applied to the full FePt Hamiltonian. The solid line indicates the numerical solution using the CSD method (see section IVB) for the FePt Hamiltonian without dipole-dipole interaction.

where $\mathbf{m}_i$ is the thermally averaged magnetization of the ith plane. The free energy is $F = -k_\mathrm{B}T \ln Z$ with the partition function $Z = \int (\prod_i d\mathbf{S}_i) e^{-\beta \mathcal{H}_{MF}}$ and $\beta = 1/k_\mathrm{B}T$.

Consider a domain wall forced into the system by appropriate boundary conditions. In a system without anisotropy a one-dimensional domain wall would develop; a state with a unique angle between all planes involved. In a MF picture it is hence sufficient to consider only three planes in order to describe the thermodynamics of the whole domain wall. Let ψ be the angle between the magnetic moments of the different planes. The thermally averaged magnetization of the ith plane is assumed to be oriented in the z-direction and is given by $\mathbf{m}_i = m_\psi \mathbf{e}_z$, with m_ψ being the magnitude of the magnetisation in a wall with angle ψ. The magnetization of the $(i-1)$th plane is then given by $\mathbf{m}_{i-1} = m_\psi (\cos\psi \mathbf{e}_z + \sin\psi \mathbf{e}_x)$ and the one of the $(i+1)$th plane has the form $\mathbf{m}_{i+1} = m_\psi (\cos\psi \mathbf{e}_z - \sin\psi \mathbf{e}_x)$ where
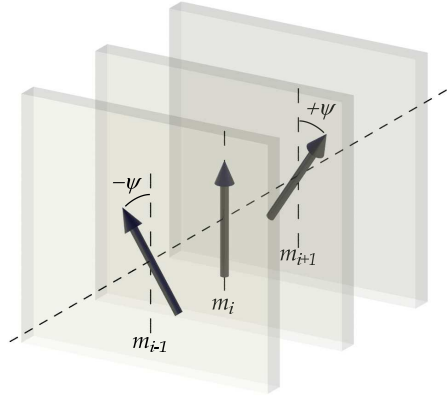

Figure 3: Sketch of the three planes under consideration. The magnetization is in the $x-z$ plane and tilted by an angle ψ between adjacent planes.

it is assumed that the magnetization is in the $x-z$ plane (see Fig. 3). With these assumptions the free energy per spin has the form

$$F(\psi) = -\frac{1}{\beta} \ln \mathrm{Tr} e^{\beta J \sum_i \mathbf{S}_i \cdot (m_\psi (4+2\cos\psi)\mathbf{e}_z)}$$
$$-\frac{1}{\beta} \ln \mathrm{Tr} e^{-\frac{\beta J}{2} \sum_i m_\psi^2 (4+2\cos\psi)}. \tag{10}$$

The free energy of the domain wall ΔF is the difference of the free energies of a system with ($F(\psi)$) and without a domain wall ($F(0)$). The integrals can be solved, resulting in the free energy (per spin) of a domain wall with angle ψ between adjacent planes

$$\Delta F = \frac{J}{2} \left(m_\psi^2 (4+2\cos\psi) - 6m_0^2 \right)$$
$$-\frac{1}{\beta} \ln \frac{\sinh(J\beta m_\psi (4+2\cos\psi))}{\sinh(6J\beta m_0)}$$
$$+\frac{1}{\beta} \ln \frac{m_\psi (4+2\cos\psi)}{6m_0}. \tag{11}$$

m_0 is the magnetisation in a system without a wall. These magnetisation values can be obtained from the MF self-consistency equation,

$$\mathbf{m}_i = \langle \mathbf{S}_i \rangle = \frac{1}{Z} \int (\prod_i d\mathbf{S}_i) \, \mathbf{S}_i \, e^{-\beta \mathcal{H}_{MF}}. \tag{12}$$

Once again solving the integral results in the thermally averaged magnetization of the i-th plane (in the z-direction) within a domain wall with angle ψ. This is given by

$$m_\psi = \mathcal{L} \left(\frac{Jm_\psi (4+2\cos\psi)}{k_\mathrm{B}T} \right) \tag{13}$$

with $\mathcal{L}(x) = \coth x - 1/x$ being the Langevin function. Note that $m_0 = m_{\psi=0}$ is the normal equilibrium magnetization. These equations for m_0 and m_ψ can be solved
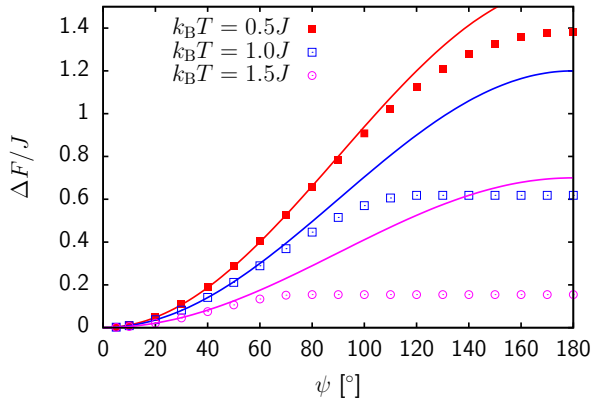
Figure 4: Angle dependence of the domain wall free energy for different temperatures. The data points are the numerical solution of Eq. (13) in connection with Eq. (11) while the solid lines represent the analytical approximation (the second part of Eq. (15))
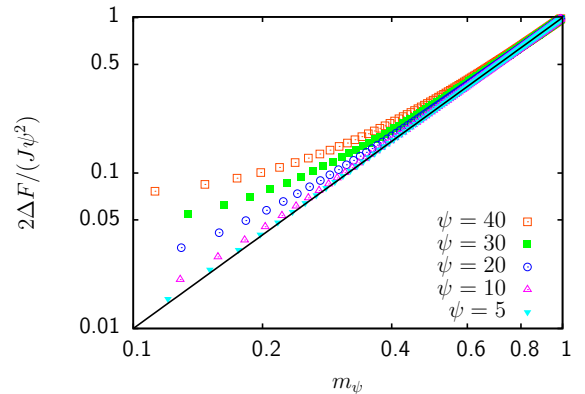

Figure 5: Magnetization dependence of the domain wall free energy for different angles ψ. The data points are from the numerical solution of Eq. (13) in connection with Eq. (11) while the black line represents the m_ψ^2-behavior (see Eq.15).

numerically and the results can be used in Eq. (11) to calculate the domain wall free energy exactly. However, in certain limits analytical solutions can be obtained as well.

In the following we will focus on the behavior of the domain wall free energy in the low temperature limit. In this limit the self-consistency equation can be expanded up to the first order in T and one obtains

$$m_\psi = \frac{1}{2} + \sqrt{\frac{1}{4} - \frac{1}{\beta J(4 + 2\cos\psi)}}. \qquad (14)$$

Using this approximation in Eq. (11) leads to an approximation for the free energy of a domain wall in the limit of small angles as well as for low temperature,

$$\Delta F \approx \frac{J}{2} m_\psi^2 \psi^2 \approx J m_\psi^2 (1 - \cos(\psi)). \qquad (15)$$

This expression for the domain wall free energy can well be compared with a micromagnetic expression for the exchange contribution to the energy density (per cross-sectional area) $\Delta F_{\text{exc}} = 2aA(1 - \cos(\psi))$, yielding a relation for the temperature-dependent exchange stiffness $A(T) = J m_\psi^2(T)/2a$ where a is the distance between adjacent planes. The main result is that the exchange stiffness scales with the square of the magnetization in the domain wall.

Fig. 4 shows a comparison of the domain wall free energy obtained from a numerical solution of the self-consistency equations with the small angle – low temperature approximation. It can be seen that in the limit of small angles the approximation coincide with the exact data. The lower is the temperature the wider is the range of validity of the approximation shown in Eq. (15).

Fig. 5 shows the scaling behavior of the domain wall free energy with the magnetization m_ψ for different angles ψ. The smaller is the angle the larger is the magnetization range where the m_ψ^2-scaling applies. The data

points represent the numerical solution while the solid line represents the scaling behavior in the low temperature limit according to Eq. (15).

IV. THE SPIN-WAVE STIFFNESS APPROACH

A. Numerical approach: Langevin dynamics simulation of spin-waves.

Another common definition of the exchange parameter is via the spin-wave (SW) stiffness. A priori it is not clear that this definition coincides with the one used in the previous section based on domain wall properties, since the equilibrium background magnetization is different in both cases. In the present section we evaluate the temperature-dependent exchange stiffness via Langevin dynamics simulations of thermally excited SW (SW Langevin), using the method outlined in Refs.[33,34]. For this purpose we simulate a generic, three dimensional ferromagnet with a Heisenberg Hamiltonian as in Eq. (1), with $d = 0$ and external applied field H parallel to the z−axis. The system size is $\mathcal{N} = 32 \times 32 \times 32$ with $T_c = 700K$ ($k_B T_c \approx 1.44J$, see, e.g. Ref. 35).

The random thermal field introduces correlated magnetization fluctuations. These can be analyzed via a Fourier analysis, both in space and time, by transforming the magnetization fluctuations $\widetilde{\mathbf{m}}(\mathbf{r}, t) = (m_x(\mathbf{r}, t), m_y(\mathbf{r}, t))$ around the equilibrium direction $\mathbf{m}_0 = (0, 0, 1)$ via a Discrete Fourier Transform $\mathcal{DFT}$,

$$\widetilde{\mathbf{m}}(\mathbf{k}, \omega_n) = \mathcal{DFT}(\widetilde{\mathbf{m}}(\mathbf{r}, t_n)). \qquad (16)$$

where $\{t_n\}$ is the discrete time and the wavevector for a finite box-shaped ferromagnet with periodic boundary conditions takes the form $k_\nu = \frac{2\pi n_\nu}{aN_\nu}$ with $n_\nu = 0, 1, \ldots, \mathcal{N}_\nu - 1$; $\nu = x, y, z$.

The power spectral density $F(\mathbf{k}, w) = |\widetilde{\mathbf{m}}(\mathbf{k}, \omega)|^2$ is presented in Fig. 6 (a) for four different characteristic temperature regions and for the fixed wavevector

$\mathbf{q} = (0, 0, \pi/(4a))$. For low temperatures the intensity of the SW modes decrease with the wavenumber k, while at high temperature there occurs a redistribution of the energy over all modes. The mode intensities are fitted by the Lorentzian profile from which the resonance frequency of each mode is extracted and finally the dispersion relation $\omega_{\mathbf{k}}$ is constructed. The corresponding dispersion relations are plotted in Fig.6(b). As expected, a softening of the SW modes with increased temperature occurs.

The low-temperature dispersion relation of spin waves is well known. It is obtained by linearizing the LLG equation around equilibrium and has the form

$$\frac{\omega_{\mathbf{k}}}{\gamma} = H + H_A + \frac{J_0}{\mu_s}\left(1 - \gamma_{\mathbf{k}}\right), \qquad (17)$$

with $J_0 = zJ$ and $\gamma_{\mathbf{k}} = z^{-1}\sum_{\boldsymbol{\delta}} e^{i\mathbf{k}\cdot\mathbf{a}_{ij}}$, where z is the number of nearest neighbors, $H_A = 2d^{(0)}/\mu_s$ is the anisotropy field. By using the SW Langevin technique we obtain an exact dispersion relation $\omega_{\mathbf{k}}$ as can be seen in Fig. 6(b). We now assume the following temperature dependent dispersion relation for the LLG Langevin simulated SW

$$\frac{\omega_{\mathbf{k}}(T)}{\gamma} = H + H_A + \frac{A(T)}{M_s(T)a^2}\left(1 - \gamma_{\mathbf{k}}\right), \qquad (18)$$

By fitting our numerical dispersion relations to this expression, we extract the temperature dependence of the micromagnetic parameter $A(T)$. Note that at high temperatures only the low frequency part of the spectrum was used, in agreement with the long-wave length interpretation of the micromagnetic exchange (3). The results are presented in Fig.1 as a function of the equilibrium magnetization $m(T) = M_s(T)/M_s(0)$. Once again, a scaling behavior $A \sim m^\kappa$ is found, coinciding with the results based on the numerical evaluation of the domain wall stiffness (see also the discussion in the next subsection).

B. Analytical approach: The Classical Spectral Density Method

We now use theoretical formalism developed in Ref.36, known as the classical spectral density method (CSDM). We will apply the CSDM to two different systems, a ferromagnet described by the generic classical Hamiltonian in Eq. (1) and to the full FePt Hamiltonian (2) without dipole-dipole interaction.

In this method one makes use of the lowering and raising operators $S_i^{\pm} \equiv S_i^x \pm S_i^y$, related to S_i^z by the identity $S_i^+ S_i^- = S^2 - (S_i^z)^2$, and of the Fourier transforms

$$\mathbf{S}_{\mathbf{k}} = \sum_j e^{i\mathbf{k}\cdot\mathbf{r}_j}\mathbf{S}_j; \; J_{\mathbf{k}} = \sum_j J_{ij}e^{-i\mathbf{k}(\mathbf{r}_i - \mathbf{r}_j)}, \qquad (19)$$
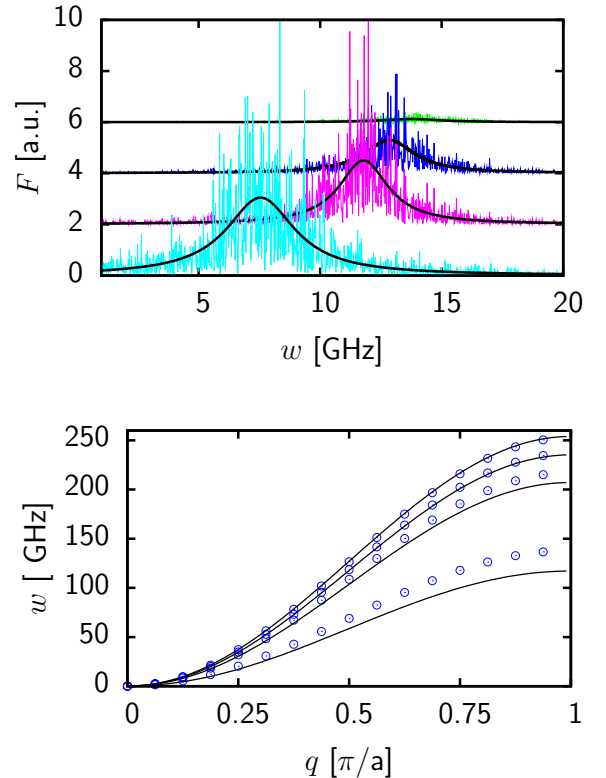

Figure 6: (a) Power spectrum density as a function of frequency for thermally excited SW in a generic Heisenberg Hamiltonian for a system of $\mathcal{N} = 32 \times 32 \times 32$ moments for various temperatures (from top to bottom) $T = T_C/70$, $T = T_C/4$, $T = T_C/2$ and $T = 0.9T_C$, for fixed wave vector $\mathbf{q} = (0, 0, \pi/(4a))$, and applied field $H_z = 1$T. (b) Dispersion relations for SWs with wavevector $\mathbf{q} = (0, 0, q)$ computed via the Langevin dynamics simulations (symbols) for the same temperatures (from top to bottom). The lines show the results obtained by the CSDM method, see section IVB.

where the zero-wave vector component reads $J_0 = \sum_j J_{ij} = zJ$, with J being the exchange coupling between first nearest neighbors (n.n.). $z = J_0/J$ can be seen as the mean coordination number with interaction coupling J. For sc lattice with only n.n. $z = 6$. By defining $\gamma_{\mathbf{q}} = z^{-1}\sum_j \eta^j e^{-i\mathbf{q}\mathbf{a}_{ij}}$ where $\mathbf{a}_{ij}$ is the relative position of considered neighbors and $\eta^i = J_{ij}/J_1$ the relative exchange strength, we can write $J_{\mathbf{q}} = J_0 \gamma_{\mathbf{q}}$. The spin variables $S_{\mathbf{q}}^{\pm}$ and $S_{\mathbf{q}}^z$ satisfy the following Poisson relations

$$\{S_{\mathbf{k}}^{\pm}, S_{\mathbf{q}}^z\} = \pm S_{\mathbf{k}+\mathbf{q}}^{\pm}, \; \{S_{\mathbf{k}}^+, S_{\mathbf{q}}^-\} = -2i\, S_{\mathbf{k}+\mathbf{q}}^z. \qquad (20)$$

In terms of these Fourier components the Hamiltonian becomes

$$\mathcal{H} = -hS_0^z - \frac{1}{2\mathcal{N}}\sum_{\mathbf{q}} J_{\mathbf{q}}\left(S_{\mathbf{q}}^+ S_{-\mathbf{q}}^- + S_{\mathbf{q}}^z S_{-\mathbf{q}}^z\right)$$
$$- \frac{1}{2\mathcal{N}}\sum_{\mathbf{q}}(d_{\mathbf{q}}^{(2)} + d^{(0)})S_{\mathbf{q}}^z S_{-\mathbf{q}}^z, \qquad (21)$$

where $h \equiv \mu_s H$, the sum in the last term is restricted to the first Brillouin zone (1BZ) of the lattice and $S_0^z = \sum_{j=1}^N S_j^z$ is the $\mathbf{k} = \mathbf{0}$ Fourier component of $S^z(\mathbf{r})$. Analogously to the exchange term, we have also defined for the two-ion anisotropy $d_{\mathbf{q}}^{(2)} = d_0^{(2)} \gamma_{\mathbf{q}}^{(\text{ani})}$ with $\gamma_{\mathbf{q}}^{(\text{ani})} = z_{\text{ani}}^{-1} \sum_j \eta_{\text{ani}}^j e^{-i\mathbf{q}\mathbf{a}_{ij}}$, $d_0^{(2)} = \sum_j d_{ij}^{(2)}$, $\eta_{\text{ani}}^i = d_{ij}^{(2)}/d_1^{(2)}$. Note that this Hamiltonian reduces to the generic one for $d_{\mathbf{q}}^{(2)} = 0$.

In CSDM one further introduces the classical spectral density $\Lambda_{AB}(\tau) \equiv i\langle\{A(\tau), B\}\rangle$ where the brackets $\langle\ldots\rangle$ denote the equilibrium ensemble average and $\{\}$ the Poisson bracket of the classical operators A and B. Then, the calculations proceed by assuming a given form (e.g. a Gaussian or a Lorentzian) for $\Lambda_{\mathbf{k}}(\widetilde{\omega})$ involving a few parameters (the frequency $\widetilde{\omega}$ is measured in the energy units μ_s/γ). The latter are obtained by solving a hierarchy of moment equations which are in turn obtained from a chain of equations for Green's functions of all orders. In terms of the spectral density $\Lambda_{AB}(\tau)$ these equations can be written as

$$\int_{-\infty}^{\infty} \frac{d\widetilde{\omega}}{2\pi} \widetilde{\omega}^m \Lambda_{AB}(\widetilde{\omega}) = -i^{m-1} \langle\{\mathcal{L}_H^m A, B\}\rangle, \quad m = 1, 2, \ldots \tag{22}$$

where $\mathcal{L}_H^m A$ stands for $\mathcal{L}_H^0 A = A, \mathcal{L}_H^1 A = \{A, \mathcal{H}\}, \mathcal{L}_H^2 A = \{\{A, \mathcal{H}\}, A\}$ and so on.

In the present case, we introduce the following spectral density

$$\Lambda_{\mathbf{k}}(\widetilde{\omega}) = i\left\langle\left\{S_{\mathbf{k}}^+(\tau), S_{-\mathbf{k}}^-\right\}\right\rangle_{\widetilde{\omega}} \tag{23}$$

$$= i \int_{-\infty}^{\infty} d\tau\, e^{i\widetilde{\omega}\tau} \left\langle\left\{S_{\mathbf{k}}^+(\tau), S_{-\mathbf{k}}^-(0)\right\}\right\rangle,$$

and assume that it can be represented approximately by one $\delta-$function

$$\Lambda_{\mathbf{k}}(\widetilde{\omega}) = 2\pi\lambda_{\mathbf{k}}\delta(\widetilde{\omega} - \widetilde{\omega}(\mathbf{k})). \tag{24}$$

This involves two unknown parameters $\lambda_{\mathbf{k}}$ and $\widetilde{\omega}(\mathbf{k})$ which are obtained by solving the equations for the first two moments. Indeed, from the zero-moment equation we have

$$\int \frac{d\widetilde{\omega}}{2\pi} \Lambda_{\mathbf{k}}(\widetilde{\omega}) = 2\mathcal{N}m, \tag{25}$$

where we have introduced the magnetization along the field direction as $m = \mathcal{N}^{-1}\langle S_0^z\rangle$. Thus, from Eq. (25) it immediately follows that $\lambda_{\mathbf{k}} = 2\mathcal{N}m$ and from the first moment equation we have

$$\int \frac{d\widetilde{\omega}}{2\pi} \widetilde{\omega}\Lambda_{\mathbf{k}}(\widetilde{\omega}) = 2m\mathcal{N}h \tag{26}$$

$$+ \frac{1}{\mathcal{N}} \sum_{\mathbf{q}} \varrho_{\mathbf{q}}^\perp \langle S_{\mathbf{q}}^+ S_{-\mathbf{q}}^-\rangle + 2\varrho_{\mathbf{q}}^\parallel \langle S_{\mathbf{q}}^z S_{-\mathbf{q}}^z\rangle,$$

where we have defined $\varrho_{\mathbf{q}}^\perp(\mathbf{k}) = 2d_{\mathbf{k}-\mathbf{q}}^{(2)} - 2d^{(0)} + J_{\mathbf{k}} - J_{\mathbf{k}-\mathbf{q}}$ and $\varrho_{\mathbf{q}}^\parallel(\mathbf{k}) = 2d_{\mathbf{q}}^{(2)} + 2d^{(0)} + J_{\mathbf{k}} - J_{\mathbf{k}-\mathbf{q}}$.

The transverse correlation function appearing on the right-hand side of Eq. (26) can be readily calculated leading to

$$\langle S_{\mathbf{k}}^+ S_{-\mathbf{k}}^-\rangle = \frac{2\mathcal{N}m}{\beta\widetilde{\omega}_{\mathbf{k}}} \equiv 2\mathcal{N}m\Omega_{\mathbf{k}}, \tag{27}$$

where we have introduced the thermally averaged occupation number

$$\Omega_{\mathbf{k}} = \frac{1}{\beta\widetilde{\omega}_{\mathbf{k}}}. \tag{28}$$

In order to compute the longitudinal correlation function in Eq. (26) one has to make use of a particular decoupling procedure (see the discussion below and in the appendix). This is the second approximation used in CSDM, in addition to that related with the choice for the form of the spectral density. In Ref. 36 (and references therein) the following approximation is used

$$\langle S_{\mathbf{k}}^z S_{-\mathbf{k}}^z\rangle \simeq \langle S_{\mathbf{k}}^z\rangle\langle S_{-\mathbf{k}}^z\rangle - \frac{1}{2}\left(1 - m^2\right)\langle S_{\mathbf{k}}^+ S_{-\mathbf{k}}^-\rangle. \tag{29}$$

Finally, defining the averaged exchange structural factors $\mathcal{T}^{(\text{ex})}$, where $\mathcal{T}^{(\text{iso})} = \mathcal{N}^{-1}\sum_{\mathbf{q}} \gamma_{\mathbf{q}}\Omega_{\mathbf{q}}$ stands for the isotropic exchange interaction and, $\mathcal{T}^{(\text{ani})} = \mathcal{N}^{-1}\sum_{\mathbf{q}} \gamma_{\mathbf{q}}^{(\text{ani})}\Omega_{\mathbf{q}}$ for the anisotropic one (two-ion anisotropy, see above). We have for the frequency dispersion relation the self-consistent equation

$$\widetilde{\omega}_{\mathbf{k}} = h + 2d^{(0)}\mathcal{K}_1(T) + 2d_0^{(2)}\mathcal{K}_2(T) + \mathcal{A}(T)J_0(1 - \gamma_{\mathbf{k}}) \tag{30}$$

where the first contribution stems from the Zeeman energy and the second from the single-ion uniaxial anisotropy energy, where

$$\mathcal{K}_1(T) = m - \frac{\Omega}{2}\left(3 - m^2\right), \tag{31}$$

with $\Omega = \mathcal{N}^{-1}\sum_{\mathbf{k}}^{1ZB}\Omega_{\mathbf{k}}$. The third term in Eq. (30) is due to the two-ion anisotropy and contributes to both the zero wavevector mode $\widetilde{\omega}_0$ and to the non-zero wavevector modes (i.e. exchange). Its temperature dependence is described by

$$\mathcal{K}_2(T) = m - \mathcal{T}^{(\text{ani})}\left(1 - m^2 + \gamma_{\mathbf{k}}^{(\text{ani})}\right). \tag{32}$$

As a result, within the CSDM approximation we recover the anisotropy field scaling with magnetization in the low temperature region. Especially for FePt, we obtain that the effective anisotropy field $h_A = 2d^{(0)}\mathcal{K}_1(T) + 2d_0^{(2)}\mathcal{K}_2(T) \approx 2d_0^{(2)}m^{\beta_A}$, where $\beta_A = 1 + d^{(0)}/d_0^{(2)} \approx 1.072$. Moreover, the micromagnetic anisotropy constant scales as 2.072, to be compared with the scaling exponent 2.1 of the anisotropy constant found experimentally[29,30] and numerically[8]. The last term in Eq. (30) is due to the

isotropic exchange interaction whose temperature dependence is given by

$$\mathcal{A}(T) = m \left(1 + m\mathcal{T}^{(\text{iso})}\right) \qquad (33)$$

In all cases the contributions $\mathcal{T}^{(\text{iso})}\gamma_{\mathbf{k}}$ and $\mathcal{T}^{(\text{ani})}\gamma_{\mathbf{k}}^{(\text{ani})}$ are due to magnon-magnon interactions as can be checked from different theoretical approaches that account for non-linear SW effects. This is discussed in the Appendix.

To solve Eq. (30), the thermally reduced magnetization value is necessary. We use the following expression, valid for arbitrary temperature, as suggested in Ref. 36,

$$m^2 = \frac{1 - 3m\Omega}{1 - m\Omega}. \qquad (34)$$

It is easy to show that it reduces to the well known expression for the reduced magnetization in the low temperature limit, $m \simeq 1 - \Omega$, for classical spin systems[37]. Consequently, Eq. (30) should be solved self-consistently together with Eq. (34). The results are plotted in Fig. 6 and compared with the SW dispersion obtained through the Langevin dynamics simulation.

Despite the assumptions, such as the δ-function for the spectral density and the decoupling procedure such as in Eq. (29), the temperature-dependent equilibrium magnetization m is well described in the low temperature region $T < T_C/4$ and in the high temperature region $T \cong T_C$, including an acceptable prediction of the Curie temperature $k_B T_C \approx 1.47J$ for the generic case[36]. At the same time in the intermediate temperature region the temperature-dependent equilibrium magnetization obtained through the CSDM approach is lower with respect to that obtained within the SW Langevin approach. This explains the deviations observed in the dispersion relation for intermediate temperature. This discrepancy, however, almost vanishes when the exchange stiffness is plotted in terms of the corresponding magnetization value m [see Figs.1,2] where the CSDM approach practically coincides with the Langevin simulations.

The low-temperature exponent for the scaling of the exchange stiffness with magnetization can be found analytically with some approximations. We will neglect the influence of the temperature dependence of the zero wavevector part $\widetilde{\omega}_0 = h + h_A(T)$ on the dispersion relation, which becomes exact in the absence of anisotropy. For the anisotropic exchange case of FePt we neglect the exchange anisotropy contribution to $\widetilde{\omega}_{\mathbf{k}}$, because $d_0^{(2)}/J_0 \ll 1$. With these approximations, the dispersion relation (Eq.30) reduces to

$$\widetilde{\omega}_{\mathbf{k}} \simeq \widetilde{\omega}_{\mathbf{0}}(T) + m\mathcal{Q}(m)J_0\left(1 - \gamma_{\mathbf{k}}\right), \qquad (35)$$

with $\mathcal{Q}(m) = 1 + m\mathcal{T}^{(\text{iso})}$. Averaging over the non-interacting magnon gas the interaction terms $\mathcal{T}^{(\text{ex})}$ and using Eq.(34), we obtain the following expression for the function $\mathcal{Q}(m)$,

$$\mathcal{Q}(m) \simeq 1 + \frac{G(\varsigma)}{W(\varsigma)}\Delta m, \qquad (36)$$

	W	G	ε	κ
sc	1.5164	0.52	0.343	1.66
bcc	1.393	0.3965	0.2847	1.715
fcc	1.3446	0.343	0.255	1.745
FePt	1.317	0.3175	0.24	1.76

Table I: Geometrical factors and values of the scaling exponents ε and $\kappa = 2 - \varepsilon$ for different lattice structures and for the particular case of the full *ab initio* parametrized FePt Hamiltonian.

where we have used the low-temperature approximation for the magnetization, i.e., $m \simeq 1 - \frac{Wk_B}{J_0}T$ and we have defined $\Delta m = 1 - m \ll 1$. We have also defined the lattice sums $W(\varsigma)$ and $G(\varsigma)$, according to

$$W(\varsigma) = \frac{1}{\mathcal{N}}\sum_{\mathbf{q}}\frac{1}{1 - \varsigma\gamma_{\mathbf{q}}}, \quad G(\varsigma) = \frac{1}{\mathcal{N}}\sum_{\mathbf{q}}\frac{\gamma_{\mathbf{q}}}{1 - \varsigma\gamma_{\mathbf{q}}} \quad (37)$$

with $\varsigma = J_0/(\widetilde{\omega}_0 + J_0)$. In the case of FePt, due to the high anisotropy contribution, we obtain $\varsigma_{\text{FePt}} \simeq 0.975$ at small temperatures and zero applied field. For other materials $d << J_0$ and $\varsigma \approx 1$ even for relatively high applied fields. The values of the geometrical parameters and scaling exponents are presented in Table I for sc, bcc, and fcc lattice structure for $\widetilde{\omega}_0 = 0$. Note that the numerical calculation of the sums should be made carefully due to the divergent contribution of the Goldstone mode. With the definitions above, we can rewrite the value of $\mathcal{Q}(m) \approx 1 + \varepsilon\Delta m = m^{-\varepsilon}$, where $\varepsilon = G(\varsigma)/W(\varsigma)$.

Analogously to the SW Langevin approach (cf. Eq. (18)) the micromagnetic exchange at low temperatures is defined by

$$A_\nu(T) \propto \mathcal{Q}(m)m^2 \propto m^{2-\varepsilon}, \qquad (38)$$

where $\nu = x, y, z$. We should note that the differences $W(\varsigma) - 1$ and $G(\varsigma)$ measure the deviation of our result from the MFA behavior and tend to zero if the number of equivalent neighbors tends to infinity ($z \to \infty$). In this case $\mathcal{Q}(m) = 1$ and we recover the MFA result $A_\nu(m) \propto m^2$. The high temperature behavior is evaluated via numerical calculation of the dependence of $\mathcal{Q}(m)$ on m. It is easy to show that near the critical temperature $T \cong T_C$ the parameter $\mathcal{Q}(m) \to 1$ recovering again the MFA result. Moreover, from Eq. (34) we get $m \sim (T - T_C)^{1/2}$ in this region, leading to a linear dependence of the exchange stiffness, in agreement with the Landau theory of phase transitions[38].

In Fig. 1 we compare the numerical solution of the complete set of self-consistent equations (30, 34) for all ranges of temperature, and the atomistic simulation results described in the previous sections. For a generic ferromagnet there is a good agreement within the three approaches, in this case the scaling is given by $A(T) \propto m^{1.66}$ and it is valid until the usual low temperature region $T < T_C/4$. It can be seen that the CSD method and SW

Langevin simulations give a very close behavior. Moreover, the SW Langevin data has a very low data dispersion.

In the special and more complex FePt case, there are two different exchange parameters, one for directions parallel to z−axis, which we call $A_\parallel$ and another for directions perpendicular to the z-axis $A_\perp$. These exchange parameters satisfy $A_\parallel(m) = A_{x(y)}(0K)m^\kappa$ and $A_\perp(m) = A_z(0K)m^\kappa$. As observed from the DW simulations[28] the temperature dependence in both directions is the same, whereas the absolute value is different. The low-temperature scaling exponent $\kappa = 1.76$ is valid approximately until $T < T_C/4$. Note that the high temperature behavior cannot be described in terms of the power scaling law.

V. CONCLUSIONS

We have introduced methods suitable for the multi-scale modeling of the temperature-dependent exchange stiffness in magnetic materials, described by Heisenberg-type spin models. The present article aims to show the capability of the calculations of exchange stiffness in principle, leaving the investigation of more complex Hamiltonians for the future. As a first step and to check in the first place the generality of the conclusions, we have used a generic spin model on a cubic lattice and a spin Hamiltonian for FePt, parameterized through the *ab initio* calculations.

In the spirit of classical approaches to the exchange stiffness, we have considered two possibilities: the domain wall and the SW approaches. It is not clear *a priori* that the two definitions give the same answer in the thermodynamical sense. Indeed, the first approach captures the thermal averaging of the micromagnetic parameters inside the long-wave-length excitations in the form of a domain wall. At the same time, the SW spectrum was evaluated as small-amplitude excitations in the whole wavevector range on the background of the saturated state. To make the situations similar and to comply with the micromagnetic interpretation of exchange, only the long-wave-length part of the SW spectrum was used at high temperatures. The results of the two numerical approaches are in agreement, and they also agree with analytical calculations based on the classical spectral density method.

Our methods allows us to obtain the low-temperature scaling behavior of the exchange stiffness with magnetization. The scaling exponent was found to be $A(T) \sim m^{1.66}$ for the generic sc lattice and $A(T) \sim m^{1.76}$ for FePt. The values of the exponents are well understood within the CSDM approach as a consequence of the linear magnetization dependence on temperature within the Heisenberg model and SW nonlinearities. The absolute value of the low-temperature exponent is defined by the geometry of the lattice. The CSDM method also clarifies the failure of the mean-field approximation to get the correct low-temperature scaling. Indeed, as is well known, the MF model does not treat correctly the correlations between different SW modes (magnon-magnon interactions). Our results show that this problem also manifests itself in the temperature dependence of the exchange stiffness.

The CSDM method adequately describes the SW dispersion relation for low temperatures only up to $T < T_c/4$. At the same time, when the exchange stiffness is represented as a function of magnetization (averaged strength of the magnetization fluctuations), it gives a satisfactory agreement with numerical approaches even at high temperatures. However, for more complex Hamiltonian models its validity region should always be checked against numerical approaches.

The SW stiffness method requires a lot of computational space for the Fourier transform in four dimensions. The use of the Fourier transform also implies a regular lattice. In spite of the fact that the definition of the exchange via the long wavelength SW stiffness is rigorous, its computational feasibility is limited. The domain wall approach, however, can be applied in arbitrary systems, including multi-phase and disordered ones.

VI. ACKNOWLEDGEMENT

APPENDIX: NON-LINEAR SPIN-WAVE EFFECTS.

Considering the simpler Hamiltonian (1) without the anisotropy contribution, the CSDM approach yields the following SW dispersion relation

$$\widetilde{\omega}_\mathbf{k} = h + m \left(J_\mathbf{0} - J_\mathbf{k} \right) + \frac{m^2}{\beta} \times \frac{1}{\mathcal{N}} \sum_\mathbf{p} \frac{J_\mathbf{p} - J_{\mathbf{k}-\mathbf{p}}}{\widetilde{\omega}_\mathbf{p}}. \quad (39)$$

The extra term in Eq. (39) with a quadratic dependence on the magnetization m is a contribution that stems from the particular (higher-order) decoupling scheme used for the longitudinal correlation function in Eq.(29). With a simpler MF theory, or random-phase approximation (RPA), or still the well known Bogoliubov-Tyablikov approximation (BTA), one obtains a linear dependence on m in the additional contribution, as will be seen shortly.

In fact, there are many prescriptions for such a decoupling scheme that is used within the Green's function (GF) approach to the calculation of the dispersion relation, the magnetization, and higher-order spin averages of a magnetic system. Indeed, within this approach one is led to apply a certain scheme for breaking high-order Green's functions into lower-order ones in order to close the system of equations which is then easily solved in Fourier space. Finding an adequate scheme for doing so has triggered many investigations each dealing with a specific situation with a particular Hamiltonian. Unfortunately, there is no general or systematic procedure. What is clear, however, is that this variety of decoupling schemes only reflects the complexity of dealing with magnon-magnon interactions and non-linear SW effects. On the other hand, a decoupling scheme that may be valid for the exchange coupling is not necessarily a good approximation for the local anisotropy contributions. Indeed, in the quantum case, the spin operators satisfy the $SO(3)$ Lie algebra and this implies that two spin operators commute when they refer to distinct lattice sites. In particular, the longitudinal and transverse motions are uncorrelated when they refer to two distinct lattice sites and they are strongly correlated otherwise. Now, when applying MF theory, RPA or the BTA approximation, it is assumed that the longitudinal and transverse motions are uncorrelated and this is a valid approximation only when they refer to distinct sites $i \neq k$. However, in the (local) anisotropy contributions these sites are identical and thus the longitudinal and transverse motions are correlated, which renders such decoupling procedures bad approximations. In Ref. 39 it was argued that one can avoid using a decoupling scheme by establishing $2S$ equations of motion for the anisotropy functions. The problem, however, with this approach is that in practice one has to specify the spin S thus limiting the calculations to a particular material. In addition, it is not obvious how to obtain the classical limit from the final results. One should also note that Devlin's approach[39] is only worth the trouble when one is interested in an arbitrary ratio $k = K/J$. However, in typical situations this ratio is of the order of 10^{-2} for bulk magneto-crystalline anisotropy.

As mentioned earlier, these various contributions that stem from different decoupling schemes are in fact due to magnon-magnon interactions and non-linear SW effects. To illustrate this idea, let us consider the simplest case of a spin Hamiltonian without the anisotropy contribution and use the Holstein-Primakoff representation for the spin operators $\mathbf{S}$. Then, the lowest-order nonlinear terms arising from the isotropic exchange interaction are the four-magnon terms as were derived by Dyson[40,41] [see also[42,43]]

$$\mathcal{H}_{ex}^{(4)} = \frac{1}{4\mathcal{N}} \sum_{\mathbf{k},\mathbf{k}',\mathbf{k}''} \left[J(\mathbf{k}) + J(\mathbf{k}+\mathbf{k}'-\mathbf{k}'') - 2J(\mathbf{k}-\mathbf{k}'') \right]$$
$$a_{\mathbf{k}}^\dagger a_{\mathbf{k}'}^\dagger a_{\mathbf{k}''} a_{\mathbf{k}+\mathbf{k}'-\mathbf{k}''}. \tag{40}$$

Applying the lowest-order RPA to this 4th-order term we obtain

$$\mathcal{H}_{ex}^{(4)} = -\frac{1}{2\mathcal{N}} \sum_{\mathbf{k},\mathbf{k}'} \left[J(\mathbf{0}) - J(\mathbf{k}) - J(\mathbf{k}') + J(\mathbf{k}'-\mathbf{k}) \right]$$
$$\langle n_{\mathbf{k}} \rangle a_{\mathbf{k}'}^\dagger a_{\mathbf{k}'}. \tag{41}$$

where $\langle n_{\mathbf{k}} \rangle$ is the thermal occupation number given by the Bose-Einstein distribution

$$\langle n_{\mathbf{k}} \rangle = \frac{1}{\exp(\beta\hbar\widetilde{\omega}_{\mathbf{k}}) - 1}.$$

In the classical limit this reduces to Eq. (28).

On the other hand, the linear SW theory yields the magnon dispersion

$$\begin{aligned} \widetilde{\omega}_{\mathbf{k}}(0) &= h + S\left[J(\mathbf{0}) - J(\mathbf{k}) \right] \\ &\equiv h + \widetilde{\omega}_{\mathbf{k}}^{ex}(0). \end{aligned} \tag{42}$$

Then, the temperature-dependent magnon dispersion is obtained by adding the contribution from the magnon-magnon interactions (41) to $\widetilde{\omega}_{\mathbf{k}}(0)$. Indeed, after taking into account the symmetry $\mathbf{k} \leftrightarrow \mathbf{k}'$ in Eq. (41) we obtain

$$\widetilde{\omega}_{\mathbf{k}}(T) = \widetilde{\omega}_{\mathbf{k}}(0) - \tag{43}$$
$$\frac{1}{\mathcal{N}} \sum_{\mathbf{p}} \left[J(\mathbf{0}) - J(\mathbf{k}) - J(\mathbf{p}) + J(\mathbf{p}-\mathbf{k}) \right] \langle n_{\mathbf{p}} \rangle,$$

which can be rewritten as [see the textbook 44, p. 256]

$$\widetilde{\omega}_{\mathbf{k}}(T) = h + \widetilde{\omega}_{\mathbf{k}}^{ex}(0) \left[1 - \frac{1}{\mathcal{N}J_0} \sum_{\mathbf{k}'} \widetilde{\omega}_{\mathbf{k}'}^{ex}(0) \langle n_{\mathbf{k}'} \rangle \right]. \tag{44}$$

This (renormalized) dispersion relation can also be derived using the technique of double-time Green's functions. Indeed, this technique yields

$$\widetilde{\omega}_{\mathbf{k}}^{free} = \mu_s H + \langle S^z \rangle \left[J(\mathbf{0}) - J(\mathbf{k}) \right] \tag{45}$$

where $\langle S^z \rangle$ is the magnetization in the direction of the field. Now, replacing the latter by

$$\langle S^z \rangle = S - \frac{1}{\mathcal{N}} \sum_{\mathbf{p}} \langle n_{\mathbf{p}} \rangle$$

and adding the magnon interaction contribution

$$\widetilde{\omega}_{\mathbf{k}}^{int} = \frac{1}{\mathcal{N}} \sum_{\mathbf{p}} \left[J(\mathbf{p}) - J(\mathbf{p}-\mathbf{k}) \right] \langle n_{\mathbf{p}} \rangle$$

yields the temperature-dependent dispersion

$$\begin{aligned} \widetilde{\omega}_{\mathbf{k}}(T) = & \; h + S\left[J(\mathbf{0}) - J(\mathbf{k}) \right] \\ & - \frac{1}{\mathcal{N}} \sum_{\mathbf{p}} \left[J(\mathbf{0}) - (\mathbf{k}) - J(\mathbf{p}) + J(\mathbf{p}-\mathbf{k}) \right] \langle n_{\mathbf{p}} \rangle \end{aligned}$$

which is just the dispersion given earlier in Eq. (43). This result simply shows that the extra term (third) in Eq. (39) is clearly due to magnon-magnon interactions.

Note that the dispersion relation in Eq. (45) is obtained within the BTA. However, it was shown by Tahir-Kheli and Callen[45–47] that the more sophisticated decoupling scheme

$$\left\langle\left\langle S_i^z S_j^+; C\right\rangle\right\rangle \underset{i\neq j}{\longrightarrow} \quad \left\langle S_i^z\right\rangle \left\langle\left\langle S_j^+; C\right\rangle\right\rangle$$
$$-\frac{\left\langle S_i^z\right\rangle}{S^2}\left\langle S_i^- S_j^+\right\rangle \left\langle\left\langle S_i^+; C\right\rangle\right\rangle$$

leads to the dispersion relation

$$\widetilde{\omega}_{\mathbf{k}} = \mu_{\mathrm{s}}H + \left\langle S^z\right\rangle\left[J\left(\mathbf{0}\right) - J\left(\mathbf{k}\right)\right] \qquad (46)$$
$$+\frac{\left\langle S^z\right\rangle^2}{\mathcal{N}S^2}\sum_{\mathbf{p}}\left[J\left(\mathbf{p}\right) - J\left(\mathbf{p} - \mathbf{k}\right)\right]\left\langle n_{\mathbf{p}}\right\rangle.$$

In the classical limit, using expression (28) for $\left\langle n_{\mathbf{p}}\right\rangle$, this dispersion relation reduces to that the in Eq. (39) obtained within the CSDM.

---

[1] W. F. Brown, *Micromagnetics* (Wiley, New York, 1963).

[2] J. Fidler and T. Schrefl, J. Phys. D: Appl. Phys. **33**, R135 (2000).

[3] J. Gonzalez, O. Chubykalo, and J. Gonzalez, in *Encyclopedia of Nanoscience and Nanotechnology*, Vol. 19, edited by E.Nalwa (American Sicentific Publishers, 2004).

[4] W. Scholz, J. Fidler, T. Schrefl, D. Suess, R. Dittrich, H. Forster, and V. Tsiantos, Comp. Mat.Sci. **28**, 366 (2003).

[5] J. Fidler, T. Schrefl, and W. Scholz, in *Handbook of Theoretical and Computational Nanotechnology*, edited by W. S. M. Rieth (American Scientific Publishers, 2006).

[6] E.D.Mee and E. D. Daniels, *Magnetic recording technology* (Springer Verlag, 1990).

[7] "http://math.nist.gov/oommf/," .

[8] O. N. Mryasov, U. Nowak, K. Guslienko, and R. W. Chantrell, Europhys. Lett. **69**, 805 (2005).

[9] A. Antal, B. Lazarovits, L. Balogh, L. Udvardi, and L. Szunyogh, Phylosoph. Magazine **88**, 2715 (2008).

[10] W. F. Brown, Phys. Rev. **130**, 1677 (1963).

[11] O. Chubykalo, R. Smirnov-Rueda, M. A. Wongsam, R. W. Chantrell, U. Nowak, and J. M. González, J. Magn. Magn. Mat. **266**, 28 (2003).

[12] G. Grinstein and R. H. Koch, Phys. Rev. Lett. **90**, 207201 (2003).

[13] D. A. Garanin, Phys. Rev. B **55**, 3050 (1997).

[14] O. Chubykalo-Fesenko, U. Nowak, R. W. Chantrell, and D. Garanin, Phys. Rev. B **74**, 094436 (2006).

[15] N. Kazantseva, D. Hinzke, U. Nowak, R. W. Chantrell, U. Atxitia, and O. Chubykalo-Fesenko, Phys. Rev. B **77**, 184428 (2008).

[16] U. Nowak, *Handbook of Magnetism and Advanced Magnetic Materials, Vol. 2, Micromagnetism* (John Wiley & Sons Ltd., Chichester, 2007).

[17] H. B. Callen, J. Phys. Chem. Solids **4**, 256 (1958).

[18] P. Asselin, R.F.L. Evans, J. Barker, R.W. Chantrell, R. Yanes, O. Chubykalo-Fesenko, D. Hinzke, U. Nowak Phys. Rev. B **82**, 054415 (2010).

[19] U. Atxitia, O. Chubykalo-Fesenko, N. Kazantseva, D. Hinzke, U. Nowak, R.W. Chantrell Appl. Phys.Lett. **91**, 232507 (2007).

[20] S. Sun, C. B. Murray, D. Weller, L. Folks, and A. Moser, Science **287**, 1989 (2000).

[21] O. N. Mryasov, V. A. Gubanov, and A. I. Liechtenstein, Phys. Rev. B **45**, 12330 (1992).

[22] V. Heine, O. N. Mryasov, and A. I. Liechtenstein, EuroPhysics Letters **12**, 545 (1990).

[23] O. N. Mryasov, A. J. Freeman, and A. I. Liechtenstein, J. Appl. Phys. **79**, 4805 (1996).

[24] O. N. Mryasov, JMMM **272-276**, 800 (2004).

[25] A. B. Shick and O. N. Mryasov, Phys. Rev. B **67**, 172407 (2003).

[26] U. Nowak, O. N. Mryasov, R. Wieser, K. Guslienko, and R. W. Chantrell, Phys. Rev. B **72**, 172410 (2005).

[27] D. Hinzke, U. Nowak, O. N. Mryasov, and R. W. Chantrell, Appl. Phys. Lett. **90**, 082507 (2007).

[28] D. Hinzke, N. Kazantseva, U. Nowak, O. N. Mryasov, P. Asselin, and R. W. Chantrell, Phys. Rev. B **77**, 094407 (2008).

[29] S. Okamoto, N. Kikuchi, O. Kitakami, T. Miyazaki, Y. Shimada, and K. Fukamichi, Phys. Rev. B **66**, 24413 (2002).

[30] J.-U. Thiele, K. R. Coffey, M. F. Toney, J. A. Hedstrom, and A. J. Kellock, J. Appl. Phys. **91**, 6595 (2002).

[31] O. Chubykalo, U. Nowak, R. Smirnov-Rueda, M. A. Wongsam, R. W. Chantrell, and J. M. Gonzalez, Phys. Rev. B **67**, 64422 (2003).

[32] N. Kazantseva, R. Wieser, and U. Nowak, Phys. Rev. Lett. **94**, 037206 (2005).

[33] O. Chubykalo, J. D. Hannay, M. A. Wongsam, R. W. Chantrell, and J. M. González, Phys. Rev. B **65**, 184428 (2002).

[34] K. Yu. Guslienko, O. Chubykalo, J. D. Hannay, and R. W. Chantrell, J. Magn. Magn. Mat. **272-276**, 251 (2004).

[35] J. G. S. Rushbrooke, G. A. Baker, *Phase Transitions and Critical Phenomena*, Vol. 3 (Academic Press,, New York, 1974).

[36] L. S. Campana, A. Caramico, D'Auria, M. D. D'Ambrosio, L. D. Cesare, G. Kamieniarz, and U. Esposito, Phys. Rev. B **30**, 2769 (1984).

[37] D.A. Garanin, Phys. Rev. B **53**, 11593 (1996).

[38] L. D. Landau and E. M. Lifshitz, *Electrodynamics of Continuous Media* (Pergamon, 1984) .

[39] J. Devlin, Phys. Rev. B **4**, 136 (1971).

[40] F. J. Dyson, Phys. Rev. **102**, 1217 (1956).

[41] F. J. Dyson, Phys. Rev. **102**, 1230 (1956).

[42] D. C. Mattis, *The theory of magnetism* (Harper and Row Pubs., 1964).

[43] Yu. A. Izyumov and Yu. N. Skryabin, *Statistical Mechanics of Magnetically Ordered Materials* (Consultants Bureau, New York, London, 1988) .

[44] Robert M. White, *Quantum Theory of Magnetism* (Springer, Berlin, Heidelberg, 1970) .

[45] R. Tahir-Kheli and H. B. Callen, Phys. Rev **135**, A679 (1964).

[46] R. Tahir-Kheli, Phys. Rev **132**, 689 (1963).   .
[47] H. B. Callen, Phys. Rev **130**, 890 (1963)